

Interfacial and Film-Formation Behaviour of Photoactive Ru^{II}-Bipyridyl-Based Metallosurfactants and a Rare Example of a Monolayer-Based Logic-Gate Approach

Prasenjit Mahato,^[a] Sukdeb Saha,^[a] Sipra Choudhury,^{*[b]} and Amitava Das^{*[a]}

Three derivatives of tris(bipyridyl)-ruthenium(II) complexes with different alkyl-chain lengths ($n\text{C}_{18}\text{H}_{37}$ (**1**), $n\text{C}_{14}\text{H}_{29}$ (**2**) and $n\text{C}_{10}\text{H}_{21}$ (**3**)) were synthesised. All these complexes behaved as an amphiphile and their surface properties were studied at the air–water interface by measuring surface pressure–area (Π – A) isotherms. The surface morphology of the resulting films at the air–water interface was also studied by using Brewster angle microscopy. Mean molecular areas of these complexes were measured from the Π – A isotherms, which were approximately 200 \AA^2 , thereby indicating a parallel arrangement of the Ru–bipyridyl moiety of the complexes. Mono- and multilayer Langmuir–Blodgett (LB) films were formed on different solid surfaces with transfer ratios close to one. Similarities in the absorp-

tion and fluorescence spectra of these amphiphiles in solution as well as in LB films deposited on a quartz surface confirmed the successful transfer of these films onto the substrates. The latter provided information about the arrangements of metallosurfactant molecules within the LB films. The two-dimensional concentrations of these films were calculated from the Lambert–Beer law as well as from the Π – A isotherm, which confirmed regular and reproducible transfer of the complex monolayers from the air–water interface onto the quartz surface. The surface morphology of these films on various substrates was characterised by atomic force microscopy. Furthermore, by oxidising the monolayer of complex **3**, a one-input sequential logic gate was constructed.

Introduction

The development of thin films and surface engineering are increasingly being acknowledged as major research interests for the generation of new molecular electronic and photonic materials.^[1] The fundamental understanding of molecular interactions and orientations in such films or surfaces are essential for developing device-quality mono- and multilayers.^[2] Generally followed procedures for fabrication of thin-film devices are vacuum deposition,^[3] spin coating,^[4] self-assembly^[5,6a] and Langmuir–Blodgett (LB) techniques.^[6,7] Among these techniques, the generation of mono- or multilayers by using the LB film technique has a special significance for developing ultrathin films of appropriately functionalised molecules with controlled thickness and well-defined molecular orientation,^[8] as these have potential applications as biosensors,^[9] gas sensors^[10] and for other high-end technological purposes.^[11] The LB technique has been effectively used to construct organised systems for efficient energy and electron transfer.^[12] Metal-containing soft materials like metallopolymer,^[13] metallomesogens^[14] and metallosurfactants^[15] take advantage of the cooperativity between transition metals and organic scaffolds to build up organised supramolecular architectures with unique geometric, redox and magnetic properties. For this, such metal-containing soft materials are to be organised in highly ordered assemblies and transferred onto surfaces. Among the metallosurfactants studied in LB films, ruthenium(II)-bipyridyl-based amphiphilic complexes have received considerable attention,^[16] owing to their rich photophysical and electrochemical properties,^[17] diversity of coordination forms,^[18] high thermal, chemical and photophysical stability as well as their solu-

bility in common solvents. LB films of different ruthenium complexes have successfully been used in making nonlinear optical (NLO) materials,^[19] light-emitting diodes (LED)^[20] and high-performance sensors.^[21]

To date, enormous efforts have been devoted to the construction of a molecular logic gate, which is an important device for information processing and computation at the molecular level.^[22] At present there are several molecules reported that can perform functions of various basic and complex logic operations, but in most cases the performance has been limited to the solution phase,^[22] which remains far from practical for applications in information technology.

For constructing solid-state molecular logic devices, the immobilisation of molecules onto solid substrates is essential. This has led to an enormous opportunity for the development of a hybrid system with a molecule fabricated on a solid surface that is capable of executing Boolean operations under the influence of certain external stimulation(s).^[23] The Langmuir–

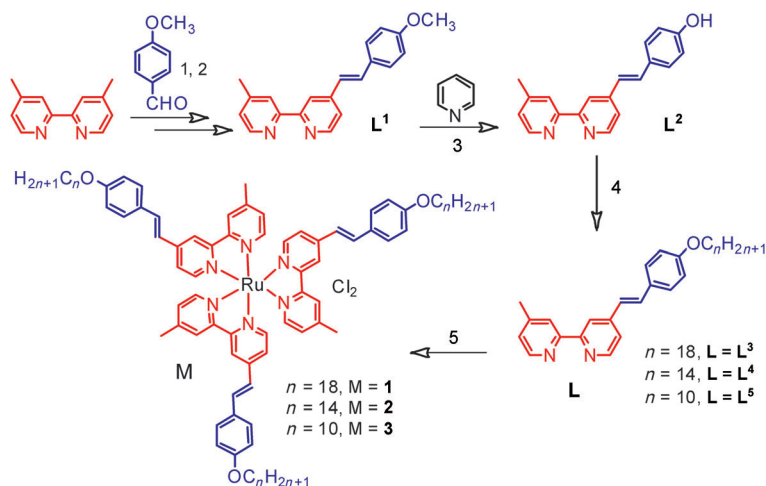
[a] P. Mahato, S. Saha, Dr. A. Das
Analytical Discipline and Centralized Instrument Facility
Central Salt and Marine Chemicals Research Institute (CSIR)
Bhavnagar, 364002, Gujarat (India)
Fax: (+91) 278-2656762
E-mail: amitava@csmcri.org

[b] Dr. S. Choudhury
Chemistry Division, Bhabha Atomic Research Center
Trombay, Mumbai, 400085 (India)
E-mail: sipra@barc.gov.in

Supporting information for this article is available on the WWW under <http://dx.doi.org/10.1002/cplu.201200207>.

Blodgett (LB) technique is one of most powerful techniques for building up nanoassemblies onto solid supports.

More recently, we have reported that a $[\text{Ru}(\text{bpy})_3]^{2+}$ -based (bpy = 2,2'-bipyridyl derivative) symmetrical amphiphilic complex (**1**) containing three $\text{C}_{18}\text{H}_{37}$ chains at equilateral positions generates interesting structures that differ in nature, size and shape depending on the polarity of the solvent environment.^[24] In the present study, we report the synthesis of two new analogous complexes (**2** and **3** in Scheme 1) having vary-



Scheme 1. Synthetic methodology that was adopted for the synthesis of complexes **1**, **2** and **3**. 1) $n\text{BuLi}$, diisopropylamine, dry THF, 0°C , 24 h; 2) POCl_3 /pyridine, 0°C , 8 h; 3) HCl , 200°C , 5 h; 4) $\text{C}_n\text{H}_{2n+1}$, DMF, K_2CO_3 , KI , 90°C , 48 h; 5) RuCl_3 , ethanol/dioxan (1:1 v/v), 85°C , 24 h.

ing alkyl-chain lengths. We have also studied various aggregated structures and films that were developed from complexes **1**, **2** and **3** under certain conditions. These metallosurfactants were found to form a stable Langmuir monolayer at the air–water interface. The morphology of the domains formed and the real-time changes of the film during compression as well as the nature of the film after collapse of the monolayer at the air–water interface were evaluated using Brewster angle microscopy (BAM). The morphologies of these monolayer films on different solid substrates were studied through atomic force microscopy (AFM). Further spectral responses on oxidation of the monolayer of **3** on a glass plate could be used for demonstrating a one-input sequential logic gate. To the best of our knowledge, this is the first study on a metallosurfactant-based LB monolayer acting as a logic device.

Results and Discussion

Amphiphilic properties

Tris(2,2'-bipyridyl)-ruthenium(II) complexes are known to be soluble in a polar solvent like water when used as the dichloride salt. This led us to synthesise $[\text{Ru}(\text{L})_3]\text{Cl}_2$ (complexes **1**, **2** and **3**; L is L^3 or L^4 or L^5 ; see Scheme 1) with the cationic Ru^{II} centre as the hydrophilic head group and the n -alkyl chain substituted in L^x ($x=3, 4$ or 5) as the hydrophobic tail group.

The chain length on the n -alkyl substituent was varied systematically in L^3 or L^4 or L^5 and thus in complex **1**, **2** and **3** from C_{18} to C_{10} , respectively, with an aim to tune the amphiphilicity of these photoactive metallosurfactants. Our earlier study reveals that **1** tends to form vesicles in a polar medium and reverse vesicles in an apolar medium.^[24] The aggregation behaviour and Langmuir monolayer formation of these complexes (**1**, **2** and **3**) at the air–water interface were studied by surface pressure versus area (Π versus A) isotherms and Brewster angle microscopy (BAM). The metallosurfactant was initially dissolved in a volatile organic solvent like chloroform. Chloroform is immiscible with water and spreads on water surfaces. Thus, a solution of the respective Ru^{II} -polypyridyl complex in chloroform was allowed to spread on the water surface in a Langmuir trough. As the chloroform evaporates, the amphiphiles form a monolayer over the water surface in which the polar Ru^{II} centre, which is hydrophilic, remains attached to the water surface, whereas the lipophilic tail points upwards. As the barriers of the trough were compressed, the surface tension (γ) at the air–water interface in the presence of the amphiphilic species was expected to decrease relative to that of the bare air–water interface ($\gamma_0 = 72 \text{ mN m}^{-1}$ at 25°C), which results in an increase in Π ($= \gamma_0 - \gamma$). Compression isotherms are plots of surface pressure (Π , in mN m^{-1}) versus mean molecular area (A , expressed in \AA^2) and provide fundamental information concerning the two-dimensional molecular organisation of the monolayer at the air–water interface, collapse pressures (Π_c), limiting areas per molecule (A_{lim}) and the average area of the molecule at the collapse of the monolayer (A_c). Simultaneously, Brewster angle microscopy evaluates film homogeneity, domain and agglomerate formation upon passing vertically polarised light through media possessing different refractive indexes.

Figure 1 shows the Π – A isotherms for complexes **1**, **2** and **3** and suggests that the three complexes are surface active. The Π – A isotherm for metallosurfactant **1** reveals that interactions

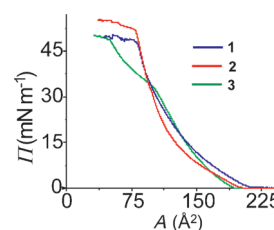


Figure 1. Langmuir–Blodgett isotherms obtained for complexes **1**, **2** and **3**.

between the molecules at the air–water interface start at 200 \AA^2 . Furthermore, two distinctly different slopes are observed in the isotherm. For the initial region, until surface pressure reaches approximately 15 mN m^{-1} , the increase in surface pressure (Π) with the change in mean molecular area (A) is not sharp. This state is called the liquid-expanded state. How-

ever, after the surface pressure reaches approximately 20 mNm^{-1} , a steep rise in the Π - A isotherm is observed (Figure 1), which could be ascribed to the formation of the liquid-compressed state.^[25] At this situation, Π rises steeply without remarkable change in A [\AA^2]. Figure 1 further reveals that the isotherm of complex **1** shows a sudden drop in surface pressure after 51 mNm^{-1} with an average area per molecule at a collapse of 125 \AA^2 (A_c). This is termed the collapse area and could be determined by extrapolating the steepest slope of the Π versus A curve (before the collapse) to zero pressure (i.e., $\Pi=0$).^[11] This collapse shows the signature of a constant pressure collapse.^[26]

The results in Figure 1 suggest that individual molecules of complex **2** start interacting at the air-water interface at an average molecular area of 196 \AA^2 (Table 1). The nature of the

Table 1. Mean molecular area and collapse pressures obtained from Langmuir-Blodgett (LB) isotherms for complexes 1 , 2 and 3 .		
Complex	Mean molecular area [\AA^2]	Collapse pressure [mNm^{-1}]
1	200	51
2	196	48
3	193	48

isotherm of this complex is similar to that of **1**, the only difference is the lower slope of the Π - A isotherm curve. The isotherm shows a high collapse pressure of 48 mNm^{-1} with a constant pressure collapse similar to that of complex **1** and with a mean area at a collapse of 106 \AA^2 (A_c). Higher collapse pressures for complexes **1** and **2** indicate the formation of a condensed and stable monolayer at the air-water interface. For complex **3**, a mean molecular area of 193 \AA^2 is evident (Figure 1), while the surface pressure is found to increase sharply until an inflection point is reached at around 32 mNm^{-1} . This indicates a mesophasic change from the liquid-expanded state to the liquid-compressed state and the monolayer collapses at 48 mNm^{-1} . Nearly analogous curves were obtained when the compression-expansion cycle was repeated. No irreversible change occurred during the second compression process. All three complexes showed constant-pressure collapse and followed the Ries mechanism of folding, bending and breaking into multilayers.^[27] The large mean molecular areas (ca. 200 \AA^2 per molecule) of these three metallo-surfactants suggest a parallel orientation of these complexes with respect to the air-water interface with alkyl chains pointing upward. These alkyl chains serve as the hydrophobic part and the central tris(2,2'-bpy)-ruthenium(II) moiety as the hydrophilic part of the amphiphilic species in the resulting film.^[8d]

Brewster angle microscopic studies

Brewster angle microscopy (BAM) is a technique that allows the in situ study of thin films at the gas-liquid or solid-gas interfaces. BAM is based on the study of the reflected light coming from an interface illuminated by a p-polarised laser

beam at the Brewster angle.^[28] When the angle of incidence of this beam is at the Brewster angle, the reflected intensity is a minimum for an air-water interface, which has a transition region where the refractive index changes smoothly from one value to another. The reflected intensity at this angle is strongly dependent on the interfacial properties, mostly when a monolayer is involved in the interface. By using BAM, the homogeneity of the film, and agglomerates and domains in films at the air-water interface could be recognised.^[29] Reflected light is a function of the orientation of the molecules in monolayer domains. BAM images were recorded at different surface pressures during the compression experiments for assessing the changes and domain formation at the air-water interface.

Selected BAM images of the air-water interface during compression experiments after spreading solutions of complexes **1**, **2** and **3** in chloroform on pure water are shown in Figure 2. Initially the blank water surface was focused in such a way that almost no reflection of p-polarised light came from the bare air-water interface and appeared black. After spreading any of these three complexes on the air-water interface, non-uniform domains with various morphology were formed, which were brighter than the black water background. Initially at zero surface pressure ($\Pi=0 \text{ mNm}^{-1}$) for complex **1**, the surface showed brighter domains of irregular shapes that indicated scattered Langmuir monolayer formation on water (dark background; Figure 2). Initially with the increase in surface pressure, movement of the domains was found to increase and it was difficult to focus all the domains available in the CCD camera at a time; however, a more uniform monolayer film was formed at $\Pi \approx 1.5 \text{ mNm}^{-1}$ as brighter domains came closer to each other. With further compression, at approximately $\Pi \approx 6 \text{ mNm}^{-1}$, a homogeneous surface with random multiple ring-shaped bright circles were observed.^[30] These rings are called Newton circles and are essentially multilayer granules that are formed by ejection of matter owing to the localised oscillation and reflect the thermodynamic instability of the film (Figure 2a).^[30] With further compression, the movement of these bright Newton circles became faster, which caused difficulties in focusing the camera on all the circles available at one time. With further lateral compression, a greater number of Newton circles over a smaller area was evident. For $\Pi \geq 20 \text{ mNm}^{-1}$, the density of these rings was even higher and they combined to form a brighter film (Figure 2a). After further compression with $\Pi \geq 30 \text{ mNm}^{-1}$, the homogeneous film became more compact and the brightness of the film was enhanced (Figure 2a). However, after the collapse pressure, the monolayer film collapsed and a rough and non-homogeneous film was observed (Figure 2a).

For complex **2**, similar changes at the air-water interface were observed (Figure 2b) as lateral compression was applied. At $\Pi \approx 1.5 \text{ mNm}^{-1}$, almost a continuous monolayer was formed and further compression led to the formation of sporadic Newton rings. However, the size of these Newton rings was larger than those of complex **1**. At $\Pi \approx 20 \text{ mNm}^{-1}$, the abundance of the rings was enhanced and they were more densely packed (Figure 2b). At even higher surface pressure ($\approx 50 \text{ mNm}^{-1}$), a rough film appeared with dark (monolayer)

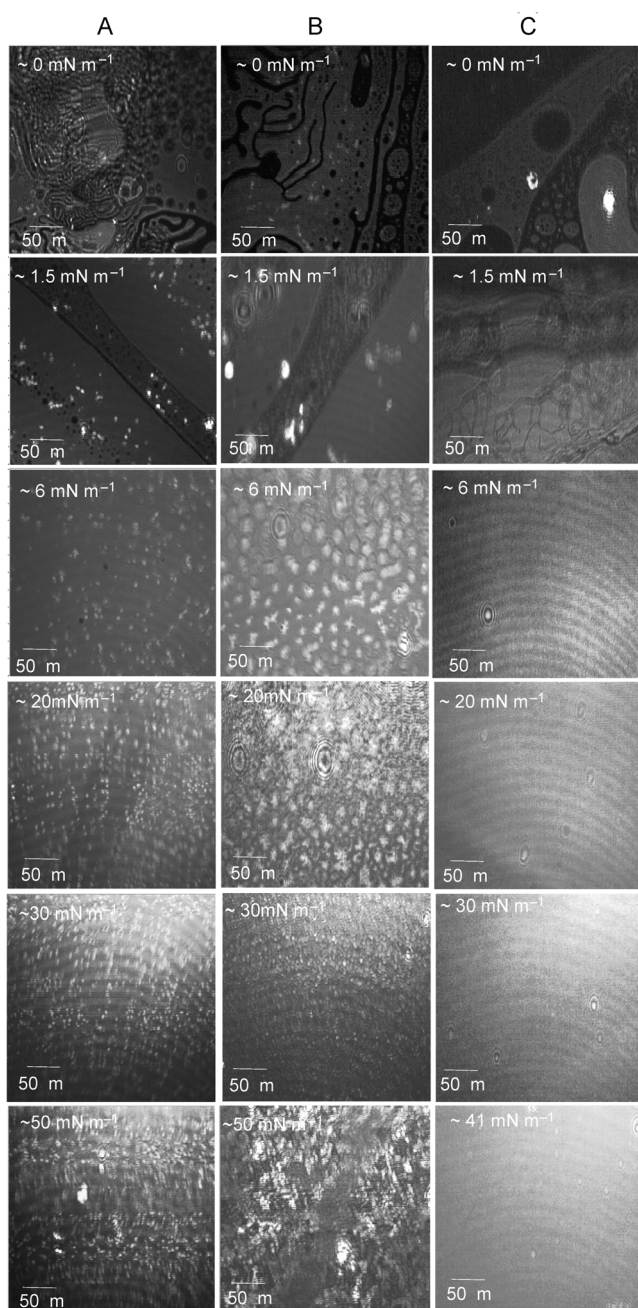


Figure 2. Selected Brewster angle micrographs for complexes A) **1**, B) **2** and C) **3** obtained at different surface pressures.

and bright (multilayer) patches, which were attributed to the collapse of the monolayer and the formation of a multilayer. Thus, on further increase in lateral compression with $\Pi > 20 \text{ mN m}^{-1}$, the interspatial distance between the resulting domains was found to be narrower and eventually led to a collapse of the monolayer at $\Pi = 50 \text{ mN m}^{-1}$ with the resulting change in morphologies. According to Vollhardt and Wiedemann,^[31] the growth of these structures occurs due to crowding of the domains from supersaturation on the surface of the surrounding phase. Again, it can also be argued that $[\text{Ru}(\text{L})_3]\text{Cl}_2$ (L is L^1 , L^2 or L^3) may remain in a dynamic equilibrium with its monohalogenated and completely solvated analogues, namely,

$[\text{Ru}(\text{L})_3(\text{H}_2\text{O})\text{Cl}]^+$ and $[\text{Ru}(\text{L})_3(\text{H}_2\text{O})_2]^{2+}$, at the air/water interface. Each of these species should exhibit distinct dipole moments that increase molecular motion. Thus, the film stabilises itself by the formation of domains that lead to a decrease in mobility.^[32] Complex **3** with the shortest chain length of the three complexes was also studied. Figure 2c reveals that this complex forms almost a uniform monolayer throughout the compression with very few Newton rings at higher pressure. At higher lateral compression, brighter film formation is evident (Figure 2c), which signifies a more compact film formation with increase in surface pressure.

Atomic force microscopic studies

Monolayer films of three amphiphilic complexes (**1**, **2** and **3**) were deposited on a hydrophilic surface (glass) at different surface pressures. The morphology of these films was analysed by atomic force microscopy (AFM). Figure 3A and B show the

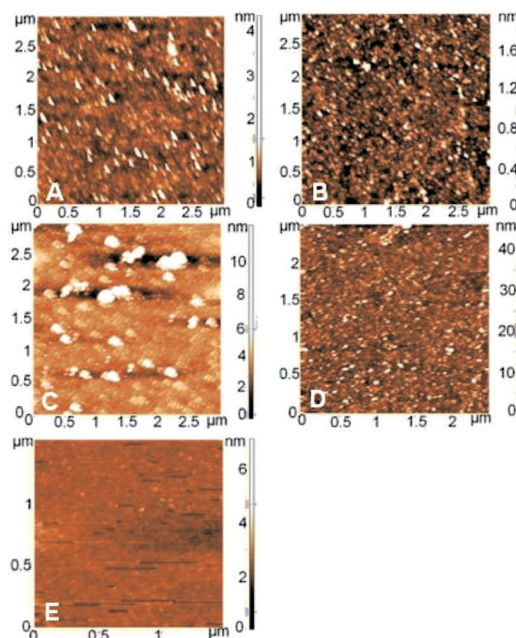


Figure 3. AFM images of the transferred film of complex **1** that was deposited at a surface pressure of A) 10 (one monolayer) and B) 30 mN m^{-1} (one monolayer) on glass; AFM images of the transferred film of complex **2** that was deposited at a surface pressure of C) 10 and D) 30 mN m^{-1} (one monolayer) on glass; E) AFM images of the transferred film of complex **3** deposited at a surface pressure of 30 mN m^{-1} (one monolayer) on glass.

AFM images of the monolayer of complex **1** deposited onto a glass surface at surface pressures of 10 and 30 mN m^{-1} , respectively. Formation of a more compact monolayer film was observed at higher surface pressure ($\Pi \approx 30 \text{ mN m}^{-1}$). This is in accordance with the Π - A isotherm of complex **1** (Figure 1); the Π - A isotherm of complex **1** is steeper at $\Pi = 30 \text{ mN m}^{-1}$ than at $\Pi = 10 \text{ mN m}^{-1}$. Thus, results obtained from each of these techniques are in good agreement. Figure 3C and D show the AFM images of monolayers of complex **2** transferred at 10 and 30 mN m^{-1} surface pressures, respectively. The AFM

image of the film, transferred at $\Pi = 10 \text{ mNm}^{-1}$, shows monolayer film formation with many bright spots (Figure 3C); whereas the film transferred at $\Pi = 30 \text{ mNm}^{-1}$ appeared more compact and contains a greater number of bright spots (Figure 3D). Figure 3E shows the AFM image of a monolayer of complex **3** transferred onto the hydrophilic glass surface at $\Pi = 30 \text{ mNm}^{-1}$. A smooth homogeneous surface indicates the formation of a compact homogeneous monolayer. These AFM results of the transferred monolayer on the solid surfaces can be correlated well with the BAM images (Figure 2) at the corresponding surface pressure, which represents the morphology of the monolayer formed at the air–water interface. BAM images (Figure 2) reveal that bright Newton rings were formed for complexes **1** and **2** at lower surface pressure (Figure 2A and B). The appearance of these Newton rings were found to increase with the increase in the surface pressure (Π) and after a certain pressure the Newton rings were so close that they formed a homogeneous film (Figure 2A and B). The AFM image of complex **1** shows a homogeneous film at 30 mNm^{-1} , which is also observed in the BAM images. The homogeneous nature of the film could be attributed to the narrower interspatial distances between the greater number of Newton rings formed at the high surface pressure. The AFM image of the transferred film of complex **1** reveals a greater number of bright spots for the film transferred at a surface pressure of 30 mNm^{-1} than that transferred at 10 mNm^{-1} , which agrees well with the morphology observed in the BAM images for the corresponding surface pressures (Figure 2). A similar increase in the density of bright spots in the AFM image of the transferred film of complex **2** with an increase in surface pressure is also evident in Figure 3 and is in good agreement with the greater number of Newton rings observed in the BAM images at 30 mNm^{-1} than that at 10 mNm^{-1} (Figure 2). At the surface pressure of 30 mNm^{-1} , the AFM image of the transferred film of **3** shows homogeneous compact morphology, which is also evident in the corresponding BAM image at a comparable surface pressure (Figure 2).

The LB films of these three complexes (complexes **1**, **2** and **3**), deposited on quartz surfaces, were further studied by absorption and fluorescence spectroscopy. Multilayer Y-type LB films of **1**, **2** and **3** were transferred onto hydrophilic quartz plates to record the electronic absorption spectra. Electronic spectra of a solution of **1** in chloroform showed three peaks at 297 ($6.5 \times 10^4 \text{ M}^{-1} \text{ cm}^{-1}$), 366 ($6.8 \times 10^4 \text{ M}^{-1} \text{ cm}^{-1}$) and 474 nm ($3.88 \times 10^4 \text{ M}^{-1} \text{ cm}^{-1}$; Figure S7 in the Supporting Information). The high-energy band at 297 nm is predominantly as a result of a ligand-centred $\pi\text{-}\pi^*$ transition, whereas the absorption at 366 nm is predominantly a result of an intraligand charge-transfer transition.^[33] The absorption band at 474 nm primarily arises as a result of a metal-to-ligand ($\text{Ru}_{\text{d}\pi} \rightarrow \text{L}_{\pi^*}$) charge-transfer transition ($^1\text{MLCT}$).^[33] In the case of a LB film, the respective absorption bands appeared at 299, 366 and 495 nm (Figure 4), respectively. This indicates that λ_{max} for the high-energy transition bands remained almost unchanged, whereas an appreciable redshift ($\approx 21 \text{ nm}$) was observed for the $^1\text{MLCT}$ band. Furthermore, this band was found to be broader for the LB film than for that in solution (Figure S7). The broadening of the

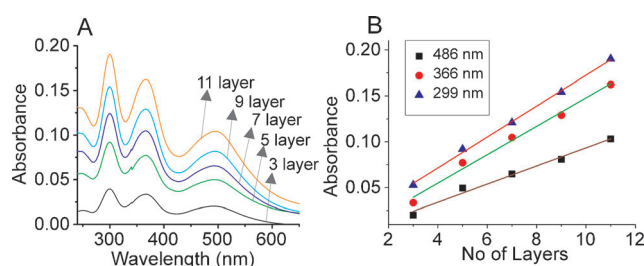


Figure 4. A) Electronic absorption spectra recorded with 3 (bottom), 5, 7, 9 and 11 (top) layers of deposition of complex **1** on a quartz substrate. B) Plot of absorbances at 299, 366 and 486 nm for varying number of deposition layers on quartz surfaces.

Table 2. Absorption maxima for the $^1\text{MLCT}$ band for complexes **1**, **2** and **3** as a solution in chloroform and as a LB film.

Complex	Absorbance maxima [nm] of $^1\text{MLCT}$ band	
	Solution	Film
1	474	495
2	471	487
3	470	487

MLCT band in the LB films, relative to that in solution, is presumably as a result of the change of the microenvironment in film compared to that in solution.

A similar redshift for the $^1\text{MLCT}$ band was also observed for complexes **2** and **3** (Table 2). This redshift can be ascribed to the aggregate nature of the molecules in the solid LB film.^[34] Alternative explanations include the change in the refractive index going from solution to the solid material.^[35a] Such a redshift in the electronic spectrum was reported earlier for Ru^{II} -polypyridyl complexes^[36] as well as other organic molecules.^[36]

The absorption spectra of the quartz plates with deposition of different multilayers (3 to 11) of complex **1** were recorded (Figure 4A) and the respective absorbance for each multilayer at 299 (ligand-centred $\pi\text{-}\pi^*$ band), 366 (intraligand charge-transfer band) and 486 nm ($^1\text{MLCT}$ band) was plotted (Figure 4B). The data in Figure 4B reveals that the absorbances at these three wavelengths follow a linear relationship with the layer number. This linear dependence indicates that in all cases the Langmuir monolayer was transferred in a regular and reproducible manner with each dipping cycle.^[37]

Similar phenomena were also observed for complexes **2** and **3** (Figure S8 and S9 in the Supporting Information). From the linear plot of absorbance versus number of layers of these metallosurfactants, the surface concentration of the LB film can be derived by using a modified expression [Eq. (1)] of the Lambert–Beer law for two-dimensional concentration:^[37,38]

$$\Gamma = D/1000\varepsilon \quad (1)$$

in which Γ , D and ε represent the surface concentration (mol cm^{-2}), absorbance per layer (AU/layer) and molar extinction coefficient ($\text{dm}^3 \text{ mol}^{-1} \text{ cm}^{-1}$), respectively, at a particular wavelength. D can be calculated from the slope of a linear plot

of absorbance versus the number of layers for a given complex. The surface concentration at the air–water interface can also be obtained from the limiting surface area (A_0 in \AA^2), which is determined by the extrapolation of the line to zero surface pressure in the Π – A isotherm following Equation (2).^[38]

$$\Gamma = 10^{16}/A_0N \quad (2)$$

in which N is Avogadro's number. The multilayer LB film-forming properties of the complexes are summarised in Table 3.

Complex	Absorbance [layer]	Surface concentration [mol cm^{-2}]	
		calculated by the Lambert–Beer law	calculated from A_0
1	8.9×10^{-3}	1.31×10^{-10}	0.83×10^{-10}
2	8.0×10^{-3}	1.26×10^{-10}	0.79×10^{-10}
3	8.74×10^{-3}	1.3×10^{-10}	0.8×10^{-10}

The surface concentrations in a LB layer as well as at the air–water interface calculated following both methods [Eqs. (1) and (2)] are consistent with each other. This further validates that the monolayers of the LB film of the respective complex are regularly transferred from the air–water interface onto the quartz substrates.

Emission spectral data of the three complexes in solution and as a LB film are summarised in Table 4. In general, the emission spectra of solutions of the complexes in chloroform and as a LB film show a broad emission band in the region 659–680 nm (Figure S10 in the Supporting Information). This emission band is attributed to the $^3\text{MLCT}$ -based excited state.^[39] The emission maxima of the LB film on the quartz surface was found to be blueshifted relative to those in solution and are attributed to the phenomenon of luminescence rigidochromism.^[40] In the fluid state, the $^3\text{MLCT}$ state of the chromophore is stabilised by reorganisation of the solvent dipoles around the chromophore dipole, whereas in a film no such solvent stabilisation is possible. The net result is the destabilisation of the $^3\text{MLCT}$ excited state in the rigid environment of the film and a shift of the emission band to higher energies.

Logic-gate behaviour of a monolayer based on complex 3

Recently, van der Boom and co-workers have reported that a silica surface functionalised with an Os^{II} -polypyridyl complex could demonstrate the function of a one-input sequential logic gate.^[23a] However, the LB film-deposition technique provides uniform arrangements of molecules with controlled thickness and well-defined molecular orientation that could not be achieved in cast films, and other thin-film techniques like spin coating, dip coating, vacuum

Complex	Emission maxima in solution [nm]	Emission maxima of LB film [nm]
1	680	659
2	680	666
3	678	665

deposition, electrodeposition and so forth. By using the LB film-deposition technique, we could easily form a monolayer of complex 3 on a glass surface that could be used for executing a chemical-input-based solid-state logic-gate operation.

The absorption spectrum of a monolayer of complex 3 on a glass substrate was recorded. This showed an absorption maximum at 487 nm. Since the glass surface is supposed to be polar, polar Ru^{II} centres of the Ru^{II} -polypyridyl-based surfactant remained in contact with the glass surface, whereas the hydrophobic tails were pointing upwards (Figure 5C). On treatment with an aqueous solution of Ce^{4+} (as ammonium ceric nitrate), Ce^{4+} ions could diffuse inside the monolayer and oxidise the Ru^{II} centre of the Ru^{II} -polypyridyl complex to Ru^{III} . This was expected to bleach the $\text{Ru}^{\text{II}}[\pi] \rightarrow \text{bpy}[\pi^*]$ -based $^1\text{MLCT}$ transition and lead to an overall decrease in the absorbance at approximately 487 nm. Partial oxidation of the Ru^{II} centres present in the monolayer led to a partial bleaching of this absorption band (Figure 5A).

Figure 5A reveals only partial bleaching of the band at 487 nm on treatment with Ce^{4+} . This suggests that only a partial oxidation of the Ru^{II} -based monolayer by Ce^{4+} could be achieved, possibly as a result of effective shielding of the $[\text{Ru}(\text{bpy})_3]^{2+}$ moiety by hydrophobic long chains. The presence or absence of an arbitrary chemical input was defined as a logical 1 or 0, respectively. The output was dependent on the formal oxidation state of the system, which was monitored by UV-visible spectroscopy. The threshold value was set at $5.0 \times$

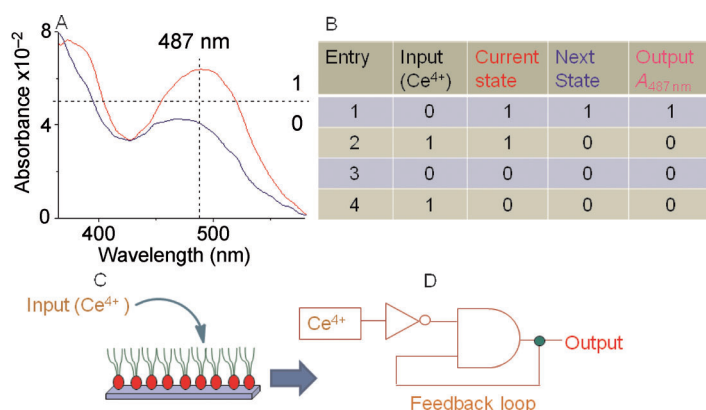


Figure 5. A) Absorption spectra of a $\text{Ru}^{2+}/\text{Ru}^{3+}$ -based LB monolayer of complex 3 (Ru^{2+} = red line, Ru^{3+} = blue line, baseline = black line). The absorption intensities at 487 nm were used as an output (0 or 1). B) Truth table with one chemical input (Ce^{4+}) with different current states ($\text{Ru}^{2+}/\text{Ru}^{3+}$). C) Sequential logic circuit based on the optical output with four combinations of one input.

10^{-2} ; output values above and below this threshold value were defined as 1 and 0, respectively (Figure 5A). Thus, a one-input sequential system was designed with Ce^{4+} ions in an aqueous solution as the input.^[23a] The four possible combinations were demonstrated with the same monolayer (Figure 5B and C). In the absence of any Ce^{4+} ions, the monolayer was in state 1 (Ru^{2+} complex existed), which was then changed to state 0 (predominant Ru^{3+} complex; Figure 5B). Since the current state is variable, the output becomes dependent on the previous input of the logic gate. Thus, based on the optical responses of the monolayer of **3** a sequential logic circuit could be constructed. Therefore, our results on molecular logic operations agreed well with the logic function demonstrated earlier using a silica-surface-grafted Os^{II} -polypyridyl complex.^[23a] The ease in developing LB films and thus the photoactive surface for executing such sequential circuit operations has significance in developing systems for practical applications.

Conclusion

Here, we have reported the synthesis of a series of symmetrical $[\text{Ru}(\text{bpy}')_3]$ -based ($\text{bpy}' = 4\text{-methyl-4'-(4-(alkoxystyryl))-2,2'-bipyridine}$) metallosurfactants with three different chain lengths: $n\text{C}_{18}\text{H}_{37}$ (**1**), $n\text{C}_{14}\text{H}_{29}$ (**2**) and $n\text{C}_{10}\text{H}_{21}$ (**3**). All three complexes form a stable monolayer at the air–water interface, which is evident from the surface pressure–area (Π – A) isotherm measurements as well as from Brewster angle microscopy. From the Π – A isotherm the average area per molecule was obtained. No significant dependence of the average area per molecule with variation in the alkyl-chain length of the metallosurfactants was observed. This indicates that the hydrophobic long-chain tails are pointed upwards from the $[\text{Ru}(\text{bpy}')_3]^{2+}$ head group with respect to the air–water interface. The change in slope in the Π – A isotherm of these complexes indicates the mesophasic changes from the liquid-expanded state to the liquid-compressed state during the compression of the monolayer. Again, high collapse pressures of these isotherms indicate the formation of homogeneous and compact monolayer film formation for the complexes. From Brewster angle microscopy, various domains formed by these metallosurfactants at low surface pressure as well as the formation of a compact monolayer with gradual increase in surface pressure were observed. These LB monolayers could be transferred successfully on the solid surfaces like glass, mica and quartz by a vertical dipping method at different surface pressures. The morphology of the transferred films was characterised by AFM and correlated with the surface morphology at the air–water interface studied by BAM. Absorption and emission spectra of the transferred films on the quartz surface were recorded, which support the uniform and regular multilayer formation on quartz surfaces. The surface concentration of the transferred film as well as at the air–water interface was calculated (Lambert–Beer law modified for two-dimensional concentration [Eq. (1)] and limiting surface area [Eq. (2)]) and both data agree with each other. More importantly, we have shown that these amphiphilic Ru^{II} complexes could be used for developing a LB film that is capable of demonstrating the novel concept of optical one-input se-

quential logic-gate operation. These results further reveal that a $[\text{Ru}(\text{bpy})_3]$ -based monolayer in the presence of suitable input(s) can speak the complex language of information technology.

Experimental Section

Materials and reagents

Analytical- and reagent-grade solvents and compounds were used for studies unless mentioned otherwise and were used as received. 4,4'-Dimethyl-2,2'-bipyridyl, 4-methoxybenzaldehyde, 1-bromooctadecane, 1-bromotetradecane, 1-bromodecane, butyllithium, diisopropylamine and ruthenium trichloride were procured from Sigma–Aldrich, whereas all other chemicals were purchased from S.D. Fine Chemicals (India). Nanopure water with a resistivity of $17.5\text{--}18\text{ M}\Omega\text{ cm}^{-1}$ was used for LB film studies. L^1 and L^2 were synthesised following previously reported procedures.^[41]

Instrumentation

Microanalyses (C, H, N) were performed using a Perkin–Elmer 4100 elemental analyzer. IR spectra were recorded as KBr pellets using a Perkin–Elmer GX 2000 spectrometer. UV-visible spectra of the complexes in solution were obtained by using a Cary 500 scan UV-Vis-NIR spectrometer. UV-visible spectra of the LB films were recorded on a Chemito UV 2600 spectrophotometer. Fluorescence spectra were recorded with a HORIBA JOBIN YVON spectrophotometer. ^1H NMR spectra were recorded on a Bruker 500 MHz FT NMR (Advance-DPX 500) spectrometer at room temperature (25°C). Tetramethylsilane (TMS) was used as an internal standard for all ^1H NMR spectroscopy studies. ESIMS measurements were carried out on a Waters QToF-Micro instrument.

Compression isotherms and deposition and LB films

Pressure–area isotherm measurements were carried out by using a computer-controlled KSV 5000 Langmuir double-barrier Teflon trough. The surface pressure was measured with a platinum Wilhelmy plate microbalance. The compression rate (the barrier speed) used was 5 mm min^{-1} at 25°C . Any impurities from the surface of the freshly poured aqueous subphase were removed by vacuum using a suction pump, after the compression of the barriers. Spreading solutions for complexes **1**, **2** and **3** with known concentration ($0.9\text{--}1.0\text{ mg mL}^{-1}$) were prepared in HPLC-grade chloroform. A known quantity (typically $80\text{--}90\text{ }\mu\text{L}$) of this solution was then allowed to spread on the clean aqueous subphase with a Hamilton microsyringe. The system was allowed to equilibrate for approximately 20 min before monolayer compression. At least three independent measurements were carried out for each experiment to ensure reproducibility of the measurements. By using the conventional vertical dipping method, LB films were transferred onto surfaces like quartz and glass. The glass and quartz slides were kept overnight in chromic acid, which was then rinsed thoroughly with Milli-Q water and immersed in an ultrasonic bath of chloroform for 10 min for appropriate cleaning. Then these slides were finally dried. The transfer ratios were 0.93 in the upward stroke and 0.78 in the downward stroke.

Brewster angle microscopy

The morphology of the Langmuir films at the air–water interface was observed by a Brewster angle microscope. BAM images of the monolayer were recorded using a nanofilm_ep3bam with a polarised Nd:YAG laser (50 mW, 532.0 nm), and a CCD camera (768×572 pixel) was used for recording images. The compression rate was 2 mm min⁻¹. The field of view was 487×387 microns and the lateral resolution was about 2 μm. The film was examined at different stages of the compression process. The length scales of the images were corrected for the angle of incidence of the incident laser beam. Images presented are typically 300×300 μm² in area. The Brewster angle (≈53.1°) was maintained between the incident p-polarised light of 532 nm and the bare air–water interface. At this stage, a negligible amount of light was reflected from the air–water interface towards the CCD camera, so the whole surface appeared black. Upon spreading the amphiphilic material at the air–water interface the refractive index of the interface was changed and a little portion (10⁻⁶ times) of the incident light was reflected, which was captured by the CCD camera.^[42] The nature of the monolayer formed was studied based on the reflected light from the interface.

Atomic force microscopy

AFM studies were carried out under ambient conditions using a scanning probe microscope NT-MDT (Ntegra Aura, Moscow) in semicontact mode using a rectangular cantilever of Si₃N₄.

Synthesis

Ligand L³: Ligand L³ was synthesised following one of our recently published procedures^[24] and was characterised using standard analytical techniques. The yield for pure L³ was evaluated based on the reactant used and was found to be 73% (476 mg, 0.89 mmol). ¹H NMR (500 MHz, CDCl₃, 25 °C, TMS): δ = 8.61 (d, ³J(H,H) = 5 Hz, 1H; 6-bpy), 8.57 (d, ³J(H,H) = 4.5 Hz, 1H; 6'-bpy), 8.48 (s, 1H; 3'-bpy), 8.25 (s, 1H; 3-bpy), 7.49 (d, ³J(H,H) = 8 Hz, 2H; 3,5-phenyl), 7.40 (d, ³J(H,H) = 16 Hz, 1H; vinyl), 7.34 (d, ³J(H,H) = 4 Hz, 1H; 5-bpy), 7.15 (d, ³J(H,H) = 3.5 Hz, 1H; 5'-bpy), 6.98 (d, ³J(H,H) = 16 Hz, 1H; vinyl), 6.91 (d, ³J(H,H) = 8 Hz, 2H; 2,6-phenyl), 3.98 (t, 2H; O-CH₂), 2.45 (s, 3H; bpy-CH₃), 1.8–1.78 (m, 2H; longchain(-CH₂)), 1.46–1.44 (m, 2H; longchain(-CH₂)), 1.26 (b, 28H; (-CH₂)₁₄), 0.88 ppm (t, 3H; longchain(-CH₃)); ESIMS (+ve mode): *m/z* (%): 541.59 (100) [M+H⁺]; elemental analysis calcd (%) for C₃₇H₅₂N₂O: C 82.17, H 9.69, N 5.18; found: C 82.1, H 9.64, N 5.15.

Ligand L⁴: The methodology used for the synthesis of L⁴ was similar to that for L³. Ligand L² (500 mg, 1.74 mmol) was dissolved in dry DMF (≈60 mL) in a two-neck round-bottomed flask under the positive pressure of N₂ gas. Finely ground pre-dried K₂CO₃ (365 mg, 2.64 mmol) was added to this with rapid stirring. 1-Bromotetradecane (0.52 mL, 1.74 mmol) was added in a dropwise manner using a syringe and the solution colour was found to change to dark yellow. To this resulting reaction mixture, finely ground pre-dried KI (439.25, 2.64 mmol in powder form) was added. Then the solution temperature was raised to 90 °C and was stirred for 48 h. Next, the reaction solution was allowed to attain room temperature (25 °C) and was filtered. The filtrate was collected and the solid residue was washed thoroughly with CH₂Cl₂. This CH₂Cl₂ washing was added to the filtrate and was evaporated to dryness through using a rotary evaporator to isolate the crude product. Then the crude product was purified by gravity chromatography using silica gel as the stationary phase and CH₂Cl₂ as the mobile phase. The isolated

yield of the purified compound (L⁴; yield was calculated based on the starting compounds) was found to be 65% (546 mg, 1.13 mmol). ¹H NMR (500 MHz, CDCl₃, TMS): δ = 8.61 (d, ³J(H,H) = 5.5 Hz, 1H; 6-bpy), 8.57 (d, ³J(H,H) = 5 Hz, 1H; 6'-bpy), 8.48 (s, 1H; 3-bpy), 8.26 (s, 1H; 3'-bpy), 7.5 (d, ³J(H,H) = 8.5 Hz, 2H; 3,5-phenyl), 7.41 (d, ³J(H,H) = 16 Hz, 1H; vinyl), 7.34 (dd, ³J(H,H)₁ = 5.5 Hz, ³J(H,H)₂ = 2 Hz, 1H; 5-bpy), 7.16 (dd, ³J(H,H)₁ = 5 Hz, ³J(H,H)₂ = 1 Hz, 1H; 5'-bpy), 6.98 (d, ³J(H,H) = 16 Hz, 1H; vinyl), 6.92 (d, ³J(H,H) = 9 Hz, 2H; 2,6-phenyl), 3.99 (t, 2H; O-CH₂), 2.45 (s, 3H; bpy-CH₃), 1.82–1.77 (m, 2H; longchain(-CH₂)), 1.46–1.43 (m, 2H; longchain(-CH₂)), 1.26 (b, 20H; (-CH₂)₁₀), 0.88 ppm (t, 3H; longchain(-CH₃)); ESIMS (+ve mode): *m/z* (%): 485.48 (100) [M+H⁺]; elemental analysis calcd (%) for C₃₃H₄₄N₂O: C 81.77, H 9.15, N 5.78, found: C 81.7, H 9.11, N 5.8.

Ligand L⁵: The synthesis and purification procedures adopted for L⁵ were similar to those mentioned for L⁴ with a necessary change in one of the reactants, namely, *n*-alkyl bromide. 1-Bromodecane (0.32 mL, 1.736 mmol) was used for this reaction instead of 1-bromotetradecane. The isolated yield of compound L⁵ (yield was calculated based on the starting compounds) was evaluated as 63% (421 mg, 0.98 mmol). ¹H NMR (500 MHz, CDCl₃, TMS): δ = 8.61 (d, ³J(H,H) = 5.5 Hz, 1H; 6-bpy), 8.57 (d, ³J(H,H) = 5 Hz, 1H; 6'-bpy), 8.48 (s, 1H; 3-bpy), 8.26 (s, 1H; 3'-bpy), 7.5 (d, ³J(H,H) = 8.5 Hz, 2H; 3,5-phenyl), 7.41 (d, ³J(H,H) = 16.5 Hz, 1H; vinyl), 7.35 (d, ³J(H,H) = 5 Hz, 1H; 5-bpy), 7.16 (d, ³J(H,H) = 4.5 Hz, 1H; 5'-bpy), 6.98 (d, ³J(H,H) = 16 Hz, 1H; vinyl), 6.92 (d, ³J(H,H) = 8.5 Hz, 2H; 2,6-phenyl), 3.99 (t, 2H; O-CH₂), 2.46 (s, 3H; bpy-CH₃), 1.82–1.77 (m, 2H; longchain(-CH₂)), 1.48–1.43 (m, 2H; longchain(-CH₂)), 1.28 (b, 12H; (-CH₂)₆), 0.88 ppm (t, 3H; longchain(-CH₃)); ESIMS (+ve mode): *m/z* (%): 429.33 (100) [M+H⁺]; elemental analysis calcd (%) for C₂₉H₃₆N₂O: C 81.27, H 8.47, N 6.54; found: C 81.2, H 8.43, N 6.5.

Complex 1: The synthesis of **1** was reported earlier and we adopted a similar methodology for the present study.^[24] The isolated yield of the **1** after purification by column chromatography was (yield was calculated based on the starting compounds) was 25% (141 mg, 0.078 mmol). ¹H NMR (500 MHz, CDCl₃, TMS): δ = 9.13–9.09 (m, 6H; 6,6'-bpy), 7.99 (d, ³J(H,H) = 17 Hz, 3H; vinyl), 7.65 (d, ³J(H,H) = 8 Hz, 6H; 3,5-phenyl), 7.59–7.5 (m, 6H; 3,3'-bpy), 7.38–7.37 (m, 3H; 5-bpy), 7.22–7.20 (m, 3H; 5'-bpy), 7.09 (d, ³J(H,H) = 16.5 Hz, 3H; vinyl), 6.92 (d, ³J(H,H) = 8.5 Hz, 6H; 2,6-phenyl), 3.98 (t, 6H; O-CH₂), 2.65 (s, 9H; bpy-CH₃), 1.78 (b, 6H; longchain(-CH₂)), 1.46–1.44 (m, 6H; longchain(-CH₂)), 1.26 (b, 84H; longchain(-CH₂)₁₄), 0.88 ppm (t, 9H; longchain(-CH₃)); ESIMS (+ve mode): ¹/₂*m/z* (%): 861.65 (15) ¹/₂[M²⁺]; elemental analysis calcd (%) for C₁₁₀H₁₅₆Cl₂N₆O₃Ru: C 74.25, H 8.67, N 4.72; found: C 74.16, H 8.81, N 4.59.

Complex 2: This complex was prepared by following the procedure that was adopted for **1**. Ligand L⁴ (220 mg, 0.454 mmol) was dissolved in ethanol/dioxan (1:1, v/v; 25 mL) mixed solvent medium. To this, RuCl₃·xH₂O (39.46 mg, 0.151 mmol) was added under an inert atmosphere and was heated at reflux for 24 h with continuous stirring. Then the reaction mixture was cooled to room temperature and was evaporated to dryness under reduced pressure. The crude solid was subjected to chromatography on alumina grade III using acetonitrile as the eluent. The major fraction was isolated and the solvent was removed to isolate the desired compound in a pure form (23% calculated based on the starting compounds; 170 mg, 0.104 mmol). ¹H NMR (500 MHz, CDCl₃, TMS): δ = 9.0 (b, 3H; 6-bpy), 8.9 (b, 3H; 6'-bpy), 7.83 (d, *J* = 16 Hz, 3H; vinyl), 7.62 (d, *J* = 6.5 Hz, 6H; 3,5-phenyl), 7.57–7.54 (m, 6H; 3,3'-bpy), 7.51 (b, 3H; 5-bpy), 7.32 (b, 3H; 5'-bpy), 7.16 (d, *J* = 17 Hz, 3H; vinyl), 6.96 (d, *J* = 7.5 Hz, 6H; 2,6-phenyl), 4.0 (t, 6H; O-CH₂), 2.61

(s, 9H; bpy-CH₃), 1.79–1.75 (m, 6H; longchain-CH₂), 1.46–1.42 (m, 6H; longchain-CH₂), 1.25 (b, 60H; longchain-(CH₂)₁₀), 0.87 ppm (t, 9H; longchain-CH₃); ESIMS (+ve mode): ¹/₂m/z (%): 777.88 (100) ¹/₂[M²⁺]; elemental analysis calcd (%) for C₉₉H₁₃₂Cl₂N₆O₃Ru: C 73.12, H 8.18, N 5.17; found: C 73.0, H 8.2, N 5.13.

Complex 3: This complex was prepared following a procedure that was adopted for complex 2. Ligand L⁵ (200 mg, 0.467 mmol) was used instead of L⁴ for the synthesis of this complex. The crude product was purified by gravity chromatography using an Al₂O₃ grade III column using a acetonitrile/chloroform (8:2, v/v) solvent mixture as the eluent. The yield of the desired complex in the pure form was found to be 25% (170 mg, 0.117 mmol) calculated based on the starting compounds used for the reaction. ¹H NMR (500 MHz, CDCl₃, TMS): δ = 9.06 (b, 6H; 6,6'-bpy), 7.96 (d, ³J(H,H) = 16 Hz, 3H; vinyl), 7.64 (d, ³J(H,H) = 8 Hz, 6H; 3,5-phenyl), 7.65–7.51 (m, 6H; 3,3'-bpy), 7.38–7.37 (m, 3H; 5-bpy), 7.21 (b, 3H; 5'-bpy), 7.09 (d, ³J(H,H) = 16 Hz, 3H; vinyl), 6.92 (d, ³J(H,H) = 8.5 Hz, 6H; 2,6-phenyl), 3.98 (t, 6H; O-CH₂), 2.65 (s, 9H; bpy-CH₃), 1.79–1.76 (m, 6H; longchain-CH₂), 1.45–1.42 (m, 6H; longchain-CH₂), 1.29 (br, 36H; longchain-(CH₂)₆), 0.88 ppm (t, 9H; longchain-CH₃); ESIMS (+ve mode): ¹/₂m/z (%): 693.86 (30) ¹/₂[M²⁺]; elemental analysis calcd (%) for C₈₇H₁₀₈Cl₂N₆O₃Ru: C 71.68, H 7.47, N 5.76; found: C 71.53, H 7.5, N 5.73.

Acknowledgements

A.D. acknowledges DST and CSIR for financial support. P.M. and S.S. acknowledge CSIR for research fellowship.

Keywords: Langmuir–Blodgett films • logic gates • monolayers • surfactants • thin films

- [1] a) A. D. Shukla, A. Das, M. E. van der Boom, *Angew. Chem. Int. Ed.* **2005**, *44*, 3237–3240; b) A. Nitzan, M. A. Ratner, *Science* **2003**, *300*, 1384–1389; c) A. Salomon, D. Cahen, S. Lindsay, J. Tomfohr, V. B. Engelkes, C. D. Frisbie, *Adv. Mater.* **2003**, *15*, 1881–1890; d) M. E. van der Boom, *Angew. Chem.* **2002**, *114*, 3511–3514; *Angew. Chem. Int. Ed.* **2002**, *41*, 3363–3366.
- [2] a) P. Zhu, H. Kang, A. Facchetti, G. Evmenenko, P. Dutta, T. J. Marks, *J. Am. Chem. Soc.* **2003**, *125*, 11496–11497; b) T. van der Boom, G. Evmenenko, P. Dutta, M. R. Wasielewski, *Chem. Mater.* **2003**, *15*, 4068–4074; c) A. Facchetti, A. Abbotto, L. Beverina, M. E. van der Boom, P. Dutta, G. Evmenenko, T. J. Marks, G. A. Pagani, *Chem. Mater.* **2002**, *14*, 4996–5005; d) G. A. Neff, M. R. Helfrich, M. C. Clifton, C. J. Page, *Chem. Mater.* **2000**, *12*, 2363–2371; e) M. S. Johal, Y. W. Cao, X. D. Chai, L. B. Smilowitz, J. M. Robinson, T. J. Li, D. McBranch, D.-Q. Li, *Chem. Mater.* **1999**, *11*, 1962–1965; f) V. Burtman, A. Zelichenok, S. Yitzchaik, *Angew. Chem.* **1999**, *111*, 2078–2082; *Angew. Chem. Int. Ed.* **1999**, *38*, 2041–2045; g) A. Ulman, *Chem. Rev.* **1996**, *96*, 1533–1554; h) H. E. Katz, W. L. Wilson, G. Scheller, *J. Am. Chem. Soc.* **1994**, *116*, 6636–6640; i) N. Nandi, D. Vollhardt, *Chem. Rev.* **2003**, *103*, 4033–4076; j) P. Ghosh, T. K. Khan, P. K. Bharadwaj, *Chem. Commun.* **1996**, 189–190; k) G. Das, P. Ghosh, P. K. Bharadwaj, U. Singh, R. A. Singh, *Langmuir* **1997**, *13*, 3582–3583; l) P. Ghosh, S. Sengupta, P. K. Bharadwaj, *Langmuir* **1998**, *14*, 5712–5718.
- [3] a) C. W. Tang, S. A. Vanslyke, *Appl. Phys. Lett.* **1987**, *51*, 913–915; b) P. E. Burrows, V. Bulovic, G. Gu, V. Kozlov, S. R. Forrest, M. E. Thompon, *Thin Solid Films* **1998**, *331*, 101–105; c) J. H. Burroughes, D. D. C. Bradley, A. R. Brown, R. N. Marks, K. Mackay, P. L. Burns, A. B. Holmes, *Nature* **1990**, *347*, 539–541; d) J. Kido, H. Hayase, K. Honogawa, K. Okuyama, K. Nagai, *Appl. Phys. Lett.* **1994**, *64*, 815–817; e) C. Vaterlein, H. Neureiter, W. Gebauer, B. Ziegler, M. Sokolowski, P. Bauerle, E. Umbach, *J. Appl. Phys.* **1997**, *82*, 3003–3013.
- [4] a) F. G. Gao, A. J. Bard, *J. Am. Chem. Soc.* **2000**, *122*, 7426–7427; b) A. Wu, D. Yoo, J. K. Lee, M. F. Rubner, *J. Am. Chem. Soc.* **1999**, *121*, 4883–4891; c) V. W. W. Yam, C. L. Chan, S. W. K. Choi, K. M. C. Wong, E. C. C. Cheng, S. C. Yu, P. K. Ng, W. K. Chan, K. K. Cheung, *Chem. Commun.* **2000**, 53–54; d) Y. G. Ma, C. M. Che, H. Y. Chao, X. M. Zhou, W. H. Chan, J. C. Shen, *Adv. Mater.* **1999**, *11*, 852–857.
- [5] a) J. Cui, Q. L. Huang, Q. W. Wang, T. J. Marks, *Langmuir* **2001**, *17*, 2051–2054; b) J. K. Lee, D. Yoo, M. F. Rubner, *Chem. Mater.* **1997**, *9*, 1710–1712; c) T. Cao, L. Wei, S. Yang, M. Zhang, C. Huang, W. Cao, *Langmuir*, **2002**, *18*, 750–753; d) M. Onoda, K. Yoshino, *J. Appl. Phys.* **1995**, *78*, 4456–4462; e) H. Hong, D. Davidov, H. Chayet, E. Z. Faraggi, M. Tarabia, Y. Avny, R. Neumann, S. Kirstein, *Supramol. Sci.* **1997**, *4*, 67–73.
- [6] a) S. Miao, H. Leeman, S. De Feyter, R. A. Schoonheydt, *Chem. Eur. J.* **2010**, *16*, 2461–2469; b) Y. Hirano, A. Maio, Y. Ozaki, *Langmuir* **2008**, *24*, 3317–3324; c) S. Ye, H. Noda, S. Morita, K. Uosaki, M. Osawa, *Langmuir* **2003**, *19*, 2238–2242; d) S. N. Sawant, M. Doble, J. V. Yakhmi, S. K. Kulshreshtha, A. Miyazaki, T. Enoki, *J. Phys. Chem. B* **2006**, *110*, 24530–24540; e) E. Arias-Marin, J. C. Arnault, D. Guillon, T. Maillou, J. Le Moigne, B. Geffroy, J. M. Nunzi, *Langmuir* **2000**, *16*, 4309–4318; f) R. Österbacka, G. Juska, K. Arlauskas, A. J. Pal, K. M. Kalman, H. Stubb, *J. Appl. Phys.* **1998**, *84*, 3359–3363; g) R. Österbacka, A. J. Pal, H. Stubb, *Thin Solid Films* **1998**, *327*, 668–670.
- [7] a) M. Hitrik, V. Gutkin, O. Lev, D. Mandler, *Langmuir* **2011**, *27*, 11889–11898; b) K. Rajesh, K. Rajendra, T. P. Radhakrishnan, *J. Phys. Chem. B* **2010**, *114*, 849–856; c) S. Miao, H. Leeman, S. De Feyter, R. A. Schoonheydt, *Chem. Eur. J.* **2010**, *16*, 2461–2469; d) Y. Hua, J. Peng, D. Cui, L. Li, Z. Xu, X. Xu, *Thin Solid Films* **1992**, *210*, 219–220; e) M. S. Weaver, D. G. Lidzey, M. A. Pavier, H. Mellor, S. L. Thope, D. D. C. Bradley, T. Richardson, T. M. Searle, C. H. Huang, H. Lui, D. Zhou, *Synth. Met.* **1996**, *76*, 91–93; f) A. P. Wu, T. Fujiwara, M. Jikei, M. A. Kakimoto, Y. Imai, T. Kubota, M. Iwamoto, *Thin Solid Films* **1996**, *284*, 901–903; g) J. M. Ouyang, L. Li, Z. H. Tai, Z. H. Lu, G. M. Wang, *Chem. Commun.* **1997**, 815–816.
- [8] a) A. Ghosh, S. Choudhury, A. Das, *Chem. Asian J.* **2010**, *5*, 352–358; b) P. Sun, D. A. Jose, A. D. Shukla, J. J. Shukla, A. Das, J. F. Rathman, P. Ghosh, *Langmuir* **2005**, *21*, 3413–3423; c) F. L. Carter, “*Molecular Electronic Devices I*” Dekker, New York, **1982**; d) A. Ulman, *An Introduction to Ultrathin Organic Films from Langmuir-Blodgett to Self-Assembly*, Academic Press, San Diego, **1991**; e) M. C. Petty, *Langmuir-Blodgett Films: An Introduction*, Cambridge University Press, New York **1996**.
- [9] a) A. A.-M. Santafe, L. J. Blum, C. A. Marquette, A. P. Girard-Egrot, *Langmuir* **2010**, *26*, 2160–2166; b) T. Govindaraju, P. J. Bertics, R. T. Raines, N. L. Abbott, *J. Am. Chem. Soc.* **2007**, *129*, 11223–11231.
- [10] a) S. Choudhury, C. A. Betty, K. G. Girija, S. K. Kulshreshtha, *Appl. Phys. Lett.* **2006**, *89*, 071914–071916; b) S. Choudhury, C. A. Betty, K. G. Girija, *Thin Solid Films* **2008**, *517*, 923–928; c) V. Saxena, S. Choudhury, S. C. Gadkari, S. K. Gupta, J. V. Yakhmi, *Sens. Actuators, B* **2005**, *107*, 277–282; d) Z. Wei, W. Xu, W. Hu, D. Zhu, *Langmuir* **2009**, *25*, 3349–3351; e) M. Schmelzer, S. Roth, C. P. Niesert, F. Effenberger, R. Li, *Thin Solid Films* **1993**, *235*, 210–214.
- [11] D. R. Talham, *Chem. Rev.* **2004**, *104*, 5479–5501.
- [12] a) J. Yoshida, K. Saruwatari, J. Kameda, H. Sato, A. Yamagishi, L. Sun, M. Corria, G. Villemurer, *Langmuir* **2006**, *22*, 9591–9597; b) T. Vuorinen, K. Kaunisto, N. V. Tkachenko, A. Efimov, H. Lemmetyinen, *Langmuir* **2005**, *21*, 5383–5390; c) K. Okamoto, M. Taniguchi, M. Takahashi, A. Yamagishi, *Langmuir* **2001**, *17*, 195–201.
- [13] a) B. J. Holliday, T. M. Swager, *Chem. Commun.* **2005**, 23–36; b) S. J. Rowan, J. B. Beck, *J. Am. Chem. Soc.* **2003**, *125*, 13922–13923; c) I. Manners, *Science* **2001**, *294*, 1664–1666; d) C. L. Fraser, A. P. Smith, *J. Polym. Sci. Part A: Polym. Chem.* **2000**, *38A*, 4704–4716.
- [14] a) E. Terazzi, S. Suarez, S. Torelli, H. Nozary, D. Imbert, O. Mamula, J.-P. Rivera, E. Guillet, J.-M. Bénech, G. Bernardinelli, R. Scopelliti, B. Donnio, D. Guillon, J.-C. Bünzli, C. Piquet, *Adv. Funct. Mater.* **2006**, *16*, 157–168; b) J. L. Serrano, T. Sierra, *Coord. Chem. Rev.* **2003**, *242*, 73–85; c) B. Donnio, *Curr. Opin. Colloid Interface Sci.* **2002**, *7*, 371–394.
- [15] a) F. D. Lesh, M. M. Allard, R. Shanmugam, L. M. Hryhorczuk, J. F. Endicott, H. B. Schlegel, C. N. Verani, *Inorg. Chem.* **2011**, *50*, 969–977; b) F. D. Lesh, R. Shanmugam, M. M. Allard, M. Lanznaster, M. J. Heeg, M. T. Rodgers, J. M. Shearer, C. N. Verani, *Inorg. Chem.* **2010**, *49*, 7226–7228; c) S. S. Hindo, R. Shakya, R. Shanmugam, M. J. Heeg, C. N. Verani, *Eur. J. Inorg. Chem.* **2009**, 4686–4694; d) R. Shakya, S. S. Hindo, L. Wu, M. M. Allard, M. J. Heeg, H. P. Hratchian, B. R. McGarvey, S. R. P. da Rocha, C. N. Verani, *Inorg. Chem.* **2007**, *46*, 9808–9818.

- [16] a) H. Zhang, C. S. Rajesh, P. K. Dutta, *J. Phys. Chem. A* **2008**, *112*, 808–817; b) M. Ledney, P. K. Dutta, *J. Am. Chem. Soc.* **1995**, *117*, 7687–7695; c) H. Monjushiro, K. Harada, M. Haga, *Langmuir* **2003**, *19*, 9226–9230; d) S. Di Bella, S. Sortino, S. Conoci, S. Petralia, S. Casilli, L. Valli, *Inorg. Chem.* **2004**, *43*, 5368–5372; e) G. Zou, K. Fang, P. S. He, W. X. Lu, *Thin Solid Films* **2004**, *457*, 365–371; f) Y. Umemura, A. Yamagishi, R. Schoonheydt, A. Persoons, F. De Schryver, *J. Am. Chem. Soc.* **2002**, *124*, 992–997; g) M. Ferreira, K. Wohnrath, A. Riul, J. A. Giacometti, O. N. Oliveira, *J. Phys. Chem. B* **2002**, *106*, 7272–7277; h) E. Holder, G. Schoetz, V. Schurig, E. Lindner, *Tetrahedron: Asymmetry* **2001**, *12*, 2289–2293; i) E. Holder, G. Trapp, J. C. Grimm, V. Schurig, E. Lindner, *Tetrahedron: Asymmetry* **2002**, *13*, 2673–2678; j) E. Holder, O. Trapp, G. Trapp, V. Marin, R. Hoogenboom, U. S. Schubert, *Chirality* **2004**, *16*, 363–368; k) B. R. Pauw, E. Holder, V. Marin, B. G. G. Lohmeijer, U. S. Schubert, *Anal. Lett.* **2007**, *40*, 163–171; l) E. Holder, M. A. R. Meier, V. Marin, U. S. Schubert, *J. Polym. Sci. Part A* **2003**, *41*, 3954–3964; m) V. Marin, E. Holder, M. A. R. Meier, R. Hoogenboom, U. S. Schubert, *Macromol. Rapid Commun.* **2004**, *25*, 793–798; n) V. Marin, E. Holder, R. Hoogenboom, U. S. Schubert, *J. Polym. Sci. Part A: Polym. Chem.* **2004**, *42*, 4153–4160; o) V. Marin, D. Wouters, S. Hoeppeener, E. Holder, U. S. Schubert, *Aust. J. Chem.* **2007**, *60*, 414–419.
- [17] a) V. Balzani, A. Juris, M. Venturi, S. Campagna, S. Serroni, *Chem. Rev.* **1996**, *96*, 759–833; b) A. Juris, V. Balzani, F. Barigeletti, S. Campagna, P. Belser, A. Vonzelewsky, *Coord. Chem. Rev.* **1988**, *84*, 85–277; c) V. Marin, E. Holder, R. Hoogenboom, E. Tekin, U. S. Schubert *Dalton Trans.* **2006**, *13*, 1636–1644; d) V. Marin, E. Holder, U. S. Schubert, *J. Polym. Sci. Part A* **2004**, *42*, 374–385.
- [18] M. Schroder, T. A. Stephenson, in *Comprehensive Coordination Chemistry*, Vol. 4 (Eds: G. Wilkinson, R. D. Gillard, J. A. McCleverty), Pergamon, Oxford, **1987**.
- [19] a) L. Boubekur-Lecaque, B. J. Coe, J. A. Harris, M. Helliwell, I. Asselberghs, K. Clays, S. Foerier, T. Verbiest, *Inorg. Chem.* **2011**, *50*, 12886–12899; b) T. Verbiest, S. Houbrechts, M. Kauranen, K. Clays, A. Persoons, *J. Mater. Chem.* **1997**, *7*, 2175–2189; c) B. W.-K. Chu, V. W.-W. Yam, *Inorg. Chem.* **2001**, *40*, 3324–3329; d) T. Nakano, Y. Yamada, T. Matsuo, S. Yamada, *J. Phys. Chem. B* **1998**, *102*, 8569–8570.
- [20] a) E. S. Handy, A. J. Pal, M. F. Rubner, *J. Am. Chem. Soc.* **1999**, *121*, 3525–3528; b) H. Rudmann, M. F. Rubner, *J. Appl. Phys.* **2001**, *90*, 4338–4345; c) F. G. Gao, A. J. Bard, *J. Am. Chem. Soc.* **2000**, *122*, 7426–7427.
- [21] a) T. Michinobu, S. Shinoda, T. Nakanishi, J. P. Hill, K. Fujii, T. N. Player, H. Tsukube, K. Ariga, *J. Am. Chem. Soc.* **2006**, *128*, 14478–14479; b) M. Ferreira, L. R. Dinelli, K. Wohnrath, A. A. Batista, O. N. Oliveira, *Thin Solid Films* **2004**, *446*, 301–306; c) M. Ferreira, A. Riul, K. Wohnrath, F. J. Fonseca, O. N. Oliveira, L. H. C. Mattoso, *Anal. Chem.* **2003**, *75*, 953–955; d) C. E. Borato, A. Riul, M. Ferreira, O. N. Oliveira, L. H. C. Mattoso, *Instrum. Sci. Technol.* **2004**, *32*, 21–30.
- [22] a) A. P. de Silva, H. Q. N. Gunaratne, C. P. McCoy, *J. Am. Chem. Soc.* **1997**, *119*, 7891–7892; b) A. P. de Silva, I. M. Dexon, H. Q. N. Gunaratne, T. Gunnlaugsson, P. R. S. Maxwell, T. E. Rice, *J. Am. Chem. Soc.* **1999**, *121*, 1393–1394; c) M. Suresh, D. A. Jose, A. Das, *Org. Lett.* **2007**, *9*, 441–444; d) M. Suresh, A. Ghosh, A. Das, *Tetrahedron Lett.* **2007**, *48*, 8205–8208; e) M. Suresh, A. Ghosh, A. Das, *Chem. Commun.* **2008**, 3906–3908; f) M. Suresh, P. Kar, A. Das, *Inorg. Chim. Acta* **2010**, *363*, 2881–2885; g) M. Kumar, R. Kumar, V. Bhalla, *Org. Lett.* **2011**, *13*, 366–369; h) M. Kumar, A. Dhir, V. Bhalla, *Org. Lett.* **2009**, *11*, 2567–2570; i) V. Bhalla, V. Vij, M. Kumar, P. R. Sharma, T. Kaur, *Org. Lett.* **2012**, *14*, 1012–1015.
- [23] a) G. de Ruiter, E. Tartakovsky, N. Oded, M. E. van der Boom, *Angew. Chem.* **2010**, *122*, 173–176; *Angew. Chem. Int. Ed.* **2010**, *49*, 169–172; b) T. Gupta, M. E. van der Boom, *Angew. Chem.* **2008**, *120*, 5402–5406; *Angew. Chem. Int. Ed.* **2008**, *47*, 5322–5326; c) J. Matsui, M. Mitsuishi, A. Aoki, T. Miyashita, *Angew. Chem.* **2003**, *115*, 2374–2377; *Angew. Chem. Int. Ed.* **2003**, *42*, 2272–2275.
- [24] P. Mahato, S. Saha, S. Choudhury, A. Das, *J. Chem. Crystallogr. Chem. Commun.* **2011**, *47*, 11074–11076.
- [25] O. N. Oliveira Jr., *Braz. J. Phys.* **1992**, *22*, 60–69.
- [26] S. Kundu, A. Datta, S. Hazra, *Langmuir* **2005**, *21*, 5894–5900.
- [27] H. E. Ries, *Nature* **1979**, *281*, 287–289.
- [28] S. Henon, J. Meunier, *Rev. Sci. Instrum.* **1991**, *62*, 936–939.
- [29] A. Gericke, A. V. Michailov, H. Huehnerfuss, *Vib. Spectrosc.* **1993**, *4*, 335–348.
- [30] J. Galvan-Miyoshi, S. Ramos, J. Ruiz-Garcia, R. Castillo, *J. Chem. Phys.* **2001**, *115*, 8178–8182.
- [31] G. Weidemann, D. Vollhardt, *Thin Solid Films* **1995**, *264*, 94–103.
- [32] J. A. Driscoll, M. M. Allard, L. Wu, M. J. Heeg, S. R. P. da Rocha, C. N. Verani, *Chem. Eur. J.* **2008**, *14*, 9665–9674.
- [33] D. A. Jose, P. Kar, D. Koley, B. Ganguly, W. Thiel, H. N. Ghosh, A. Das, *Inorg. Chem.* **2007**, *46*, 5576–5584.
- [34] F. W. Vergeer, X. Chen, F. Lafalet, L. De Cola, H. Fuchs, L. Chi, *Adv. Funct. Mater.* **2006**, *16*, 625–632.
- [35] a) A. A. Marti, J. L. Colon, *Inorg. Chem.* **2010**, *49*, 7298–7303; b) Y. Chen, W.-C. Xu, J.-F. Kou, B.-L. Yu, X.-H. Wei, H. Chao, I.-N. Ji, *Inorg. Chem. Commun.* **2010**, *13*, 1140–1143.
- [36] a) B.-K. An, S.-K. Kwon, S.-D. Jung, S. Y. Park, *J. Am. Chem. Soc.* **2002**, *124*, 14410–14415; b) S. Verma, A. Ghosh, A. Das, H. N. Ghosh, *J. Phys. Chem. B* **2010**, *114*, 8327–8334.
- [37] T. Taniguchi, Y. Fukasawa, T. Miyashita, *J. Phys. Chem. B* **1999**, *103*, 1920–1924.
- [38] B. W.-K. Chu, V. W.-W. Yam, *Inorg. Chem.* **2001**, *40*, 3324–3329.
- [39] S. Verma, P. Kar, A. Das, H. N. Ghosh, *Chem. Eur. J.* **2011**, *17*, 1561–1568.
- [40] a) V. W.-W. Yam, B. Li, Y. Yang, B. W.-K. Chu, K. M.-C. Wong, K.-K. Cheung, *Eur. J. Inorg. Chem.* **2003**, 4035–4042; b) T. G. Kotch, A. J. Lees, *Inorg. Chem.* **1993**, *32*, 2570–2575; c) S. A. Moya, R. Schmidt, U. Muller, G. Frenzen, *Organometallics* **1996**, *15*, 3453–3463.
- [41] M. A. Hayes, C. Meckel, E. Schatz, M. D. Ward, *J. Chem. Soc. Dalton Trans.* **1992**, 703–708.
- [42] D. Hoenig, D. Moebius, *J. Phys. Chem.* **1991**, *95*, 4590–4592.

Received: August 10, 2012

Revised: September 21, 2012

Published online on October 30, 2012